LA-UR- 01-6750

LA-UR-

Approved for public release; distribution is unlimited.

c.1

Title: PHOTONUCLEAR PHYSICS IN RADIATION TRANSPORT: II. IMPLEMENTATION

Author(s): WHITE, M.C.
LITTLE, R.C.
CHADWICK, M.B.
YOUNG, P.G.
MACFARLANE, R.E.

Submitted to: NUCLEAR SCIENCE AND ENGINEERING

Photonuclear Physics in Radiation Transport:

II. Implementation

M.C. White and R.C. Little

Applied Physics Division, University of California

Los Alamos National Laboratory, Los Alamos, NM 87545

M.B. Chadwick, P.G. Young, and R.E. MacFarlane

Theoretical Division, University of California

Los Alamos National Laboratory, Los Alamos, NM 87545

Abstract

This is the second of two consecutive papers presented. In the first paper, we described model calculations and nuclear data evaluations of photonuclear reactions on isotopes of C, O, Al, Si, Ca, Fe, Cu, Ta, W, and Pb, for incident photon energies up to 150 MeV. This paper describes the steps taken to process these files into transport libraries and to update the Monte Carlo N-Particle (MCNP™) and MCNPX™ (eXtended) radiation transport codes to use tabular photonuclear reaction data. The evaluated photonuclear data files are created in the standard Evaluated Nuclear Data File (ENDF) format. These files must be processed by the NJOY data processing system into A Compact ENDF (ACE) files suitable for radiation transport calculations. MCNP and MCNPX have been modified to use this new data in a self-consistent and fully integrated manner.

Verification problems were used at each step along the path to check the integrity of the methodology. The resulting methodology and tools provide a comprehensive system for using photonuclear data in radiation transport calculations. Also described are initial validation simulations used to benchmark several of the photonuclear transport tables.

I. Introduction

Photonuclear physics, until recently, has remained a strangely neglected subject of study in radiation transport computations. Libraries of *e*valuated *n*uclear *d*ata *f*iles (ENDF), such as the U.S. ENDF/B cross-section libraries [1], have not previously included evaluated photonuclear cross-section data although the capability to do so has been in place. Neither have the standard radiation transport codes included a comprehensive capability to utilize such tabulated data. While it is true that photonuclear reactions are typically negligible in transport simulations involving more dominant nuclear reactions (e.g. fission, fusion, or high-energy ion transport problems), photonuclear reactions are the primary source of nuclear particles in transport simulations of electron/photon showers. For this class of simulation problem, a key process has been missing.

We present here two consecutive papers describing work at Los Alamos National Laboratory to develop a photonuclear physics capability in our nuclear modeling, data processing and radiation transport codes. The first paper [2] describes the evaluation methods, including nuclear model calculations, used to produce evaluated photonuclear

cross-section data in the ENDF format. Results were presented for photons with incident energies up to 150 MeV on twelve isotopes: ^{12}C, ^{16}O, ^{27}Al, ^{28}Si, ^{40}Ca, ^{56}Fe, ^{63}Cu, ^{181}Ta, ^{184}W, and $^{206,207,208}Pb$. These isotopes are representative of materials found in accelerator components, collimators and beam-shaping devices, beam-stops, bremsstrahlung conversion targets, shielding, as well as elements abundant in human tissue, and comprise a useful library for many simulations. This second paper describes the processing path from ENDF library to ACE transport library (the standard data files used by MCNP and MCNPX)); the extensions to the MCNP [3] and MCNPX [4] codes to use the data; and a set of validation simulations benchmarking the new data. (Discussions within this paper using the acronym MCNP(X) indicate applicability to both MCNP and MCNPX.) Parts of this work have been published in a conference proceedings [5] and as part of one of the authors thesis [6].

There are two principal reasons why photonuclear capabilities have not previously been included in radiation transport codes through the use of evaluated data libraries: (1) experimental photonuclear data from different laboratories (e.g. data from measurement programs at Livermore, Saclay and Illinois) often show discrepancies that must be resolved in the evaluation process; and (2) there are few measurements of the energy- and angle-dependent spectra of secondary particles emitted in photonuclear reactions. Most of the existing spectral measurements are for bremsstrahlung photon sources and are only useful for integral testing. Only measurements from monoenergetic sources give emission spectra directly useful for cross-section evaluations. Because radiation transport codes need double-differential cross-section data, the widely available

photonuclear data compilations, such as those of Dietrich and Berman [7] and Varlamov et al. [8], are not immediately useful in a transport context. This is where the evaluation methodology described in the previous paper fills in the holes in measurements by using nuclear model calculations to calculate missing cross sections and provide emission spectra. These cross sections and spectra are calculated in a self-consistent manner and then validated through comparisons with measured values. The final complete evaluations provide the data necessary to perform radiation transport simulations.

A number of researchers from laboratories in Japan (JAERI, Tokyo), South Korea (KAERI, Taejon), Russia (IPPE, Obninsk and Moscow State University, Moscow), China (CIAE, Beijing), Brazil (University of Sao Paulo, Sao Paulo) and the United States (LANL and BNL) have recently worked on the development of evaluated photonuclear data for transport applications. The efforts described by our two papers have been made in coordination with this International Atomic Energy Agency (IAEA) Coordinated Research Project (CRP) entitled "Compilation and Evaluation of Photonuclear Data for Applications" [9]. The final report [10] from this project documents over 160 photonuclear evaluations. The isotopes chosen for inclusion represent those materials important in neutron radiation shielding design and radiation transport analyses; calculations of absorbed dose in the human body; physics and technology of fission and fusion reactors; activation analysis; safeguards and inspection technologies; nuclear waste transmutation; and astrophysical nucleosynthesis.

While this pair of papers is the first to present photonuclear reaction analysis using evaluated data via the ENDF format, it is important to note that previous works have included photonuclear reactions in transport simulations using other methodology. The studies mentioned here are by no means a comprehensive review but are intended to provide a feel for what has been done in past. Two approaches have dominated past efforts. The first approach is the use of intranuclear cascade codes to compute photonuclear reactions "on-the-fly" during a simulation. The works of Alsmiller et al. [11]; Gabriel [12]; Fasso, Ferrari, and Sala [13,14]; and, Mokhov et al. [15] are particularly noteworthy. The primary advantage of this approach is the ability to compute reactions on almost any target isotope over a wide range of incident photon energies. The primary disadvantage is that the computational accuracy, comparing computed to measured cross sections, can vary greatly due to the generalized nature of the model, especially in isotopic or energy regimes outside the primary focus area of the model. It is worth observing that Fasso [14] mitigates this problem by the use of experimental measurements where available.

The second approach has been various ad-hoc methodologies to use tabular data. One of the most common has been to use an electron/photon transport code to compute the photon flux within a volume of interest. This flux is folded with a photoneutron production cross section to calculate a neutron source term. This source term, with a suitable emission distribution, is then used as a source in a neutron transport code. Notable examples of this approach include the work of Chadwick et al. [16]; Swanson [17,18], McCall et al. [19]; Gallmeier [20]; and, Vertes and Ridikus [21]. The last two

examples are particularly noteworthy. Gallmeier modified MCNP and Vertes and Ridikus modified both MCNP and MCNPX to use tabulated data to compute neutron production and analytic expressions to compute emission spectra to perform coupled electron/photon/neutron transport. The work presented in this paper extends this approach to its logical conclusion. We present herein a formalized methodology for the production, processing and usage of tabular data in transport simulations. The primary advantage of this approach is that each tabular data set is produced to agree as closely as possible with measured data. The disadvantage is that a tabular data set must be created for every material of interest. However, the IAEA library will extend the 12 isotopes presented in the current work into a set that should be sufficient for almost any application. This larger library is currently undergoing review and testing.

This paper is organized as follows. Section II describes the processing and storage of the photonuclear data library including some discussion of the philosophy of data storage as driven by transport simulation needs. Several developments were necessary to the NJOY data processing code in order to process the photonuclear ENDF files into transport tables. Section III describes the updates and extensions to the MCNP and MCNPX codes that were necessary to use the data in a transport simulation. This includes discussion of issues related to code set-up and storage, user interface, sampling algorithms, biasing for variance reduction, and reporting of results. Section IV describes the results of several benchmark problems used to validate several of the data sets. Our conclusions are given in Section V.

II. Radiation Transport Data

Radiation transport codes need complete data. Complete implies the inclusion of interaction data for all materials in the geometry modeled by the simulation with reaction rates and emission spectra coupling all physical channels between particle species over the energy range of interest. Data are rarely, if ever, complete. In practice, codes use data that are "good enough." It is noteworthy that the evaluated photonuclear data sets presented in the first paper are complete and include production cross sections and emission spectra for all possible reaction channels, not just neutrons. These new data enable more accurate coupling between particles and represent a significant improvement in the state-of-the-art for radiation transport simulations.

One of the most powerful, though often overlooked, features of the MCNP(X) codes is the use of a standardized methodology for storing and utilizing interaction data. This provides the ability to use data from a wide variety of sources. For example, neutron data is created in the ENDF format by several organizations around the world. Data from any of these libraries can be processed using the NJOY data processing system and the resultant ACE transport tables can be used in MCNP(X). This allows the expert user to create data sets using the best available information for their purpose. The primary goal of this work was to establish a standardized methodology for storing and utilizing tabular photonuclear data.

The issue of storage was a key question to be decided in the early stages of this project. Photon interaction data already exist in the form of photoatomic interaction data. Photoatomic interactions are mainly characterized by elemental features, specifically the number and distribution of electrons around the atom and the charge of the nucleus. Photonuclear interactions are characterized by isotopic features, i.e. the number of neutrons and protons in the nucleus. Additionally, evaluated photonuclear data are updated one at a time, as needed for a particular isotope. Updates of photoatomic, electron and atomic relaxation data are usually done all at once in order to provide a self-consistent set of atomic libraries. With these and other factors in mind, it was decided that the current photoatomic format and data should be unchanged and that photonuclear data should be stored separately.

After deciding that photonuclear data should be stored separately, it was necessary to create a new table format for the data. The photonuclear process involves an incident photon exciting a nucleus with the subsequent emission of nuclear particles. It is expected that photonuclear reactions produce secondary particles with emission spectra similar to neutron-induced nuclear reactions. Therefore, the same data formats and sampling laws that are used to describe secondary emission for incident neutrons may be used for incident photons. The neutron class 'n' ACE table and the "ace" routines within MCNP(X) have a distinguished history of simulating particle emission from neutron collisions. The new class 'u' ACE table [22] draws on this history for storing and sampling photonuclear interactions. It stores the standard data necessary for transport and reaction calculations; i.e. the total cross section, the secondary particle production

cross sections, the individual channel cross sections with related secondary yields, the secondary particle emission spectra and reaction multipliers of interest, e.g. heating values.

The NJOY data processing system [23] has been the standard code used to process ENDF formatted data into transport data for many transport codes. The ENDF format is designed to contain interaction information in a compact, precise manner. This is rarely the form needed for efficient transport algorithms. NJOY is capable of processing ENDF format data into a wide variety of other formats including the ACE format used by MCNP(X). Beginning with NJOY99 [24], the NJOY system has included updates to process photonuclear data in ENDF format into ACE class 'u' tables.

The twelve LANL photonuclear evaluations have been processed using NJOY99.5 to create the LA150U class 'u' ACE library [25]. These tables are ready for use in the photonuclear enabled versions of MCNP(X). The modifications in MCNP(X) necessary to sample photon collisions, including both photoatomic and photonuclear events, are the subject of the next section.

III. Implementation

Extensive modifications were necessary in order to load, sample and report information about photonuclear collisions in MCNP(X). The user interface required new

constructs to allow specification of two photon interaction tables for each material component. The sampling routine required revisions to use the total photon cross section, photoatomic plus photonuclear, for calculating the distance-to-collision. The collision routine required additional interaction routines to include production of secondary particles from photonuclear collisions. The new routines also required integration with the existing variance reduction schemes, standard tallies and user output summary information. These modifications have been completed and are available beginning in MCNP release 4C2 and MCNPX beta release 2.2.3. Each of these modifications is discussed in more detail below. This discussion presumes the reader is familiar with the standard MCNP(X) features.

The decision to store photonuclear and photoatomic data in separate tables required the extension of the material specification card in the MCNP(X) input deck. The material card now recognizes ZAIDs with photonuclear IDs, e.g. 24u, as part of the component specification. Also, the material library ID for photonuclear tables may be set using the new pnlib=ID option. These two features extend the standard options available for neutron, electron and photoatomic tables. As before, ACE tables are selected for a material by finding an exact match to a given component ZAID; a match to the component ZA and library ID; the first available match to the component ZA and an appropriate table type; or, setting a fatal error state; in that order respectively.

Electron/photon simulations have a complete set of data for elements up to Z of 94. Neutron simulations have a fairly complete set of data for most isotopes and/or

elements in this range. However, since there is not a neutron data set for every isotope/element, neutron simulations typically use "good enough" approximations of materials. Therefore, material specification for problems involving neutron transport has been dominated by the selection of the neutron tables with the assumption that the corresponding photon and electron tables will be available. The addition of a sparse set of photonuclear tables complicates the material specification problem.

The issue is how to specify a material to use the best set of neutron and photonuclear data when the data sets may not include tables for all the same isotopes/elements. For example, natural tungsten is composed of five isotopes. The standard neutron libraries have tables for only four of the five. Typically, a MCNP(X) material specification calls for the four existing tables in their natural proportions and splits the atom fraction of the fifth isotope among them. The correct elemental photoatomic and electron table is attached to each for the four isotopic constituents. However, the current set of photonuclear tables have data for only one isotope of tungsten. It would be counter-productive to force the material specification to use only one isotope of tungsten because that was the only photonuclear table available. This problem will continue to exist as long as there is a mismatch between the neutron and photonuclear tables available.

The photonuclear isotope override card, labeled by MPN in an input deck, provides a solution whereby photonuclear material components may use a different ZA than that in use for electron, photoatomic and neutron tables. After the material card has

defined each component, typically based on the best set of neutron tables, a MPN card can be used to specify, possibly different, the components used to select photonuclear tables. The combination of a M and MPN card will allow users to select the best available neutron and photonuclear tables independently. Returning to the example above, the material card selects the four neutron tables as the best description of natural tungsten. The photonuclear isotope override card allows the user to specify each material component to use the one photonuclear table.

The photonuclear isotope override card provides a method for another interesting capability. At present, only 12 photonuclear tables are available. The MPN card does not restrict the user's choice of a substitute table. It is therefore possible to make substitutions between elements, e.g. substitute ^{207}Pb for ^{209}Bi. Any substitution should be chosen with care but this can be a useful technique to estimate the effect of a material component for which a table does not currently exist. Lastly, a zero value turns off photonuclear interactions in the material component. Full documentation of the changes in the material interface is available [26] as well as a primer for using this new capability [27].

Given the complexity of choosing appropriate tables, the interface described above is considered only an interim measure. As new capabilities for sampling tabular data appear in MCNP(X), the task of material specification will become even more complicated. Future work has been proposed to create a material module where the user would specify the components independently for each type of data table as well as the

true material composition. One could eventually envision specifying a molecular or elemental photoatomic, electron and thermal-neutron data sets and isotopic neutron, photonuclear and proton data sets.

In the past, MCNP(X) has sampled the distance-to-collision for photon interactions based solely on the total photoatomic cross section as that was all that was available. Below the photonuclear threshold, this is correct and above the threshold this is typically a negligible error. Only in the vicinity of the giant dipole resonance is the photonuclear cross section more than one percent of the total photon interaction cross section. Even in the resonance, it is only a few percent of the total. For this reason, using the total photoatomic interaction cross section to sample the distance-to-collision has not been unreasonable. Now, when photonuclear physics is enabled, the distance-to-collision is calculated from the more accurate total photon interaction cross section.

Once a photon has reached a collision site, both photoatomic and photonuclear secondary particles may be sampled. How this occurs is tightly coupled to the variance reduction scheme in use. First, consider the case of pure analog Monte Carlo. In this case, the initial logical decision is to choose either a photonuclear or photoatomic interaction. If the even is determined to be a photoatomic collision, it is sampled using the photoatomic interactions as previously established. Otherwise, the event is determined to be a photonuclear interaction and the code then loops through each possible secondary particle type and samples an integer number of particles to be emitted, possibly zero, based on the ratio of the particle production cross section to the total

photonuclear cross section. The emission energy and angle for each secondary particle is sampled independently from the available reactions. This is the standard sampling procedure used by MCNP(X) for neutron collisions and preserves the correct distribution statistically though not at a specific collision.

Because of its small cross section, a photonuclear interaction is a rare event. Given that these interactions are the primary source of nuclear particles that may be the focus of a given simulation, it is useful to have biasing techniques to sample them more often. Two biasing techniques are recommended for use in photonuclear simulations. These are photon collision splitting and weight windows.

Photon collision splitting is a biasing technique whereby the photon is split in two at each collision site. One photon undergoes a photoatomic interaction; the other undergoes a photonuclear interaction. Each has its weight updated to match the probability of the respective interaction type. This is a new feature for use with photonuclear collisions. It relies on the same concept underlying both implicit capture and forced collisions.

Weight windows are a particle population control method. Because of the low probability of producing secondary particles from photonuclear interactions, any biasing technique that produces more of them can also produce intensely different particle weights. In order to limit such effects, weight windows force particles into a weight range by splitting or rouletting particles outside of that range. The photonuclear collision

routine will always split or roulette the number of secondary particles such that they are in the appropriate weight range as specified by the current weight window.

While other biasing methods have also been made to work, the two outlined above are the only ones recommended. When weight windows are not used, the photonuclear collision routine will produce secondary particles and then subject them to roulette, i.e. termination, based on the current weight cutoff. Remember that the weight cutoff is modified by the ratio of the neutron importance in the current cell to the neutron importance in the source cell. This is an obscure feature inherited from the codes neutron transport origins and create unintended consequences when using geometry importance's with weight cutoffs.

Because the secondary particle production from photonuclear interactions is performed inline, it is automatically accounted for in the requested tallies. No additional information or action is required on the part of the user, nor within the code. All of the standard tallies, including point detectors, are available. Note that the routine to calculate the probability of a secondary neutron or photon scattering in a certain direction (used by the point detectors and dxtran spheres) has been updated to allow the photonuclear reaction types used within the LA150 library. Use of other data sets may require additional modifications. The code will give a bad trouble error and exit upon seeing a next-event reaction type that has not been fully implemented and verified. This does not affect transport, only next event estimators.

Additional information has been added to the print tables to reflect photonuclear interactions. This includes global and cell-by-cell statistics on photon loss due to photonuclear absorption; global and cell-by-cell statistics on photonuclear production of secondary particles; and, cell-by-cell, nuclide-by-nuclide statistics on photonuclear interactions. This new information supplements existing tables and should be familiar to users.

The capability to sample tabular photonuclear physics has been successfully integrated into MCNP and MCNPX. These codes are being distributed through the normal distribution centers. While fully integrated into the transport sections of the code, some additional work is still necessary. The "ptrac" routines need to be updated to include photonuclear events, the plotting routines need to be updated to plot the photonuclear cross sections and the tally multiplier card (FM) needs to be able to access photonuclear reaction data. These features will be addressed in future code releases.

IV. Validation

This section reviews the initial validation benchmarks performed as part of the process of implementing the photonuclear physics capability. Almost every previous effort to estimate photoneutron production has been benchmarked to experimental data published by Barber and George [28]. The Barber and George paper is exceptionally well written, documenting the key aspects of their experiment and results and reporting

there data in a manner well suited for comparison with calculations. For this reason it was chosen as the starting point for validating the current photonuclear physics implementation.

The Barber and George experiments measured total neutron yields of several materials bombarded with electrons of various incident energies. Of interest to the current work, measurements were made on aluminum, carbon, copper, lead and tantalum targets. Measurements were reported as the number of neutrons emitted from the sample per electron incident. The reported values accounted for detector efficiencies and background. This makes direct comparison of measured and calculated values possible as the number of neutrons escaping from the surface per electron incident on the target can be tallied using standard features of the MCNP(X) codes.

The experimental measurements were made using the Stanford Mark II Accelerator during the late 1950's. They followed a series of experiments to characterize the electron beam. The incident electron beam was very well understood. The target was located in a Lucite vacuum chamber surrounded by paraffin moderator. Enriched BF_3 proportional counters in the paraffin were used for neutron detection and the neutron detection efficiency was measured. Barber and George estimate their absolute accuracy as +/-15%. The targets were 4.5 inches square and of varying thickness. Because of the way in which the measurements were analyzed and reported, the only portion of the experiment necessary to model is the electron beam incident on the target. The number of neutrons escaping the target per incident electron is tallied and compared to the

experimental value. Simulations of these measurements were run using MCNP version 4C2. Each simulation was run until the Monte Carlo statistical error was negligible. Figures 1 through 13 show comparisons of experimental to calculated values. The numeric data are available in Appendix A.

The overall agreement between the calculated and measured values is good. This work, as represented by both papers, has been a difficult endeavor due to the sparse availability of measurements available for use in creating and validating the data sets and there use. Most of the validation calculations are within 25% of the experimental results. The results outside this range involve either thinner targets or points closer to the energy thresholds both conditions that are inherently difficult to calculate. It should be stated that the calculations generally underestimate the experimental values. However, this disagreement may be due to other causes. It is unknown if there were possible systematic errors in the experimental measurements. Because of the integral nature of the experiment and the corresponding simulation, these results are sensitive to the electron transport process, to bremsstrahlung production and to the photon transport process. Further, electro-disintegration effects that may be important in thin targets are ignored.

The results for aluminum, carbon, lead and tantalum were obtained from calculations with data tables for each of the major isotopes of the element. As seen in Figure 1, calculations for aluminum are in reasonable, within 25%, agreement with the experimental values. Figure 2 shows a similar level of agreement for the carbon target except for the lowest energy measurement. This may be because of interactions with

carbon-13 which is not included in the calculation and has a neutron production threshold of 4.9 MeV. As the incident energy increases, the effect of this minor isotope decreases and the results are in better agreement. The results for lead are shown in Figures 3 through 7. The calculated values for lead are remarkably consistent in their match to the experimental data and all within the 25% expected error bounds. The results for tantalum are shown in Figure 8 and again, with the exception of the lowest energy point, are in good agreement.

The results for the thick copper targets shown in Figures 9 through 12 present a consistent picture of reasonable agreement. These results were obtained from calculations using only photonuclear data available for ^{63}Cu, i.e. ignoring all effects of ^{65}Cu (30.83 atom %). Similar to previous results, the largest disagreement is seen at the lowest energies. The Cu-A target shown in Figure 13 presents the greatest enigma of the current results. This is a thin (0.1 radiation length) copper target. One hypothesis for the disagreement between measured and calculated results is that the calculation does not include electro-disintegration effects. In general, the results for copper show an increase in disagreement as the energy increases. This may be an effect of ignoring ^{65}Cu.

The overall agreement between the experimental data and the calculations is good except that the calculated results are consistently low. Three reasons are hypothesized. First, systematic errors in the data tables may result in low production cross sections. This is unlikely for reasons shown in the first paper, i.e. agreement with available thin-target cross-section measurements. Second, systematic errors in the experiment or

analysis may have led to elevated reported values. This cannot be checked. Future experiments may reveal more information. Third, systematic errors in the bremsstrahlung cross sections may result in low photon production. This may be checked through benchmarking photon production to measurements.

V. Conclusions

The work presented here describes efforts to update the MCNP and MCNPX codes to make use of newly available evaluated photonuclear data files and to validate the neutron production from photonuclear interactions for several new data files. Twelve evaluated data files have been described in the first of these two related papers [2] and we have presented here validation results for seven of those files. We have shown that the LA150U data library and the MCNP(X) codes can provide neutron production predictions with approximately 25% uncertainty. This provides an important new simulational capability for a number of applications including radiation shielding and photonuclear production of particles such as neutrons.

We reiterate that a suite of over 160 evaluated photonuclear data files has been compiled by the International Atomic Energy Agency [10]. The IAEA files will provide data tables for most isotopes of general interest. Part of the future work will be to process the IAEA evaluations into an ACE class 'u' library for use with MCNP(X).

We emphasize the need for the community to help provide validation testing for this new capability. Now that the simulation capability exists, it is hoped that more benchmarks experiments will be undertaken. In particular, there is a need to validate the other particle production and emission spectra for this capability in addition to more thorough validation of the neutron production capability.

VI. Acknowledgements

Parts of this work were performed by Morgan White while he was still a graduate student. He would like to acknowledge the support of the Department of Energy and the Oak Ridge Institute for Science and Engineering for their support under the Nuclear Engineering Fellowship program. The efforts to develop the evaluated nuclear data files at the Los Alamos National Laboratory were supported by funding from the Accelerator Production of Tritium project with special thanks to Dr. Laurie Waters. Grateful thanks are offered for useful discussions with Drs. Stephanie Frankle, Grady Hughes, Larry Cox, Dick Prael and Tom Brown.

VI. References

1. V. McLane, C.L. Dunford and P.F. Rose, eds. *ENDF-102 Data Formats and Procedures for the Evaluated Nuclear Data File ENDF-6.* BNL-NCS-44945. Brookhaven National Laboratory: Upton, NY, 1997.

2. M.B. Chadwick, R.E. MacFarlane, P.G. Young, M.C. White and R.C. Little. "Photonuclear Physics in Radiation Transport: I. Cross Sections and Spectra," *Nuclear Science and Engineering.* To be published consecutively with this paper.

3. J.F. Breismeister, ed. *MCNP - A General Monte Carlo N-Particle Transport Code.* LA-13709-M. Los Alamos National Laboratory: Los Alamos, NM, 2000.

4. L.S. Waters, ed. *MCNP - A General Monte Carlo N-Particle Transport Code.* LA-13709-M. Los Alamos National Laboratory: Los Alamos, NM, 2000.

5. M.C. White, M.B. Chadwick and R.C. Little. "Photonuclear Physics in MCNP(X)," in *Proceedings of the ANS 3rd International Topical Meeting on Nuclear Applications of Accelerator Technology*, Long Beach, California, November 14-18, 1999, pp. 515-519, VanTuyle, G., Ed., American Nuclear Society, La Grange Park, IL, 1999.

6. White, M.C. *Development and Implementation of Photonuclear Cross-Section Data For Mutually Coupled Neutron-Photon Transport Calculations in the Monte Carlo N-Particle (MCNP) Radiation Transport Code.* University of Florida: Gainesville, Florida, 2000.

7. S.S. Dietrich and B.L. Berman. "Atlas of Photoneutron Cross Sections Obtained with Monoenergetic Photons," *Atomic Data and Nuclear Data Tables.* Vol. 38, No. 2, pp. 199-338, 1988.

8. A.V. Varlamov, V.V. Varlamov, D.S. Rudenko and M.E. Stepanov. *Atlas of Giant Dipole Resonance Parameters and Graphs of Photonuclear Reaction Cross Sections.* INDC(NDS)-394. International Atomic Energy Agency: Vienna, Austria, 1999.

9. P. Oblozinsky, ed. "Compilation and Evaluation of Photonuclear Data for Applications," in *Summary Report of IAEA 1st Research Coordination Meeting.* INDC(NDS)-364. International Atomic Energy Agency: Vienna, Austria, 1998.

10. P. Oblozinsky, ed. *Handbook on Photonuclear Data for Applications: Cross-Sections and Spectra.* IAEA-TECDOC-1178. International Atomic Energy Agency: Vienna, Austria, 2000.

11. R.G. Alsmiller, Jr., T.A. Gabriel and M.P. Guthrie. "The Energy Distribution of Photoneutrons Produced by 150-MeV Electrons in Thick Beryllium and Tantalum Targets," *Nuclear Science and Engineering.* Vol. 40, No. 3, pp. 365-374, 1970.

12. T.A. Gabriel. "Intermediate-Energy (40 MeV<or approximately= E{sub gamma }<or approximately=400 MeV) Photonuclear Interactions," *Physical Review C (Nuclear Physics).* Vol. 13, No. 1, pp. 240-244, 1976.

13. A. Fasso, A. Ferrari and P.R. Sala. "Designing Electron Accelerator Shielding with FLUKA," in *Proceedings of the 8th International Conference on Radiation Protection and Shielding*, Arlington, Texas, April 24-28, 1994, pp. 643-649, American Nuclear Society, La Grange Park, IL, 1994.

14. A. Fasso, A. Ferrari and P.R. Sala. "Total Giant Resonance Photonuclear Cross Sections for Light-Nuclei: A Database for the FLUKA Monte Carlo Transport Code," in *Proceedings of the 3rd Specialists Meeting on Shielding Aspects of Accelerators, Targets, and Irradiation Facilities (SATIF-3)*, Tohoku University, Sendai, Japan, May 12-13, 1997, pp. 61-74, Organization for Economic Cooperation and Development (OECD) Nuclear Energy Agency, Paris, France, 1997.

15. N.V. Mokhov, S.I. Striganov, A. VanGinneken, S.G. Mashnik, A.J. Sierk and J. Ranft. "MARS Code Developments," in *Proceedings of the 4th Specialists Meeting on Shielding Aspects of Accelerators, Targets, and Irradiation Facilities (SATIF-4)*, Knoxville, Tennessee, September 14-16, 1998, Organization for Economic Cooperation and Development (OECD) Nuclear Energy Agency, Paris, France, 1998.

16. M.B. Chadwick, T.H. Brown and R.C. Little. "Photoneutron Production in Electron Beam Stop for Dual Axis Radiographic Hydrotest Facility (DARHT)," in *Proceedings of the 1998 ANS Topical on Radiation Protection and Shielding*, Nashville, Tennessee, April 19-23, 1998, pp. 356-363, American Nuclear Society, La Grange Park, IL, 1998.

17. W.P. Swanson. "Calculation of Neutron Yields Released by Electrons Incident on Selected Materials," *Health Physics*. Vol. 35, No. 2, pp. 353-367, 1978.

18. W.P. Swanson. "Improved Calculation of Photo-Neutron Yields Released by Incident Electrons," *Health Physics*. Vol. 37, No. 3, pp. 347-358, 1979.

19. R.C. McCall, P.R. Almond, J.A. Devanney, E.G. Fuller, G.R. Holeman, L.H. Lanzl, H. Ing and W.P. Swanson. *Neutron Contamination from Medical Electron Accelerators.* NCRP Report No. 79. National Council on Radiation Protection and Measurements: Bethesda, Maryland, 1984.

20. F.X. Gallmeier. "Photoneutron Production in MCNP4a," in *Proceedings of the 1996 ANS Topical on Radiation Protection and Shielding*, No. Falmouth, Massachusetts, April 21-25, 1996, pp. 780-786, American Nuclear Society, La Grange Park, IL, 1996.

21. P. Vertes and D. Ridikas. "Some Test Calculations with the IAEA Photonuclear Data Library," in *Proceedings of the International Conference on Nuclear Data for Science and Technology,* Tsukuba, Japan, October 7-12, 2001, Nuclear Data Center, Japan Atomic Energy Research Institute, Ibaraki-ken, Japan, 2001.

22. White, M.C. *Class 'u' ACE Format – Photonuclear Data.* Memorandum X-5:MCW-00-86(U). Los Alamos National Laboratory: Los Alamos, NM, 2000.

23. MacFarlane, R.E. and Muir, D.W. *The NJOY Nuclear Data Processing System, Version 91.* LA-12740-M. Los Alamos National Laboratory: Los Alamos, NM, 1994.

24. MacFarlane, R.E. *The NJOY Nuclear Data Processing System, Version 99.* http://t2.lanl.gov/codes/njoy99/ (accessed December 10, 2001). Los Alamos National Laboratory: Los Alamos, NM, 2000.

25. White, M.C. *Release of the LA150U Photonuclear Data Library.* Memorandum X-5:MCW-00-87(U). Los Alamos National Laboratory: Los Alamos, NM, 2000.

26. White, M.C. *User Interface for Photonuclear Physics in MCNP(X).* Memorandum X-5:MCW-00-88(U). Los Alamos National Laboratory: Los Alamos, NM, 2000.

27. White, M.C. *A Brief Primer for Simulating Photonuclear Interactions with MCNP(X).* Memorandum X-5:MCW-00-89(U). Los Alamos National Laboratory: Los Alamos, NM, 2000.

28. W.C. Barber and W.D. George. "Neutron Yields from Targets Bombarded by Electrons," Physical Review. Vol. 116, No. 6, pp. 1551-1559, 1959.

Figure 1. Neutron Yield per Electron Incident on the Al-I Target

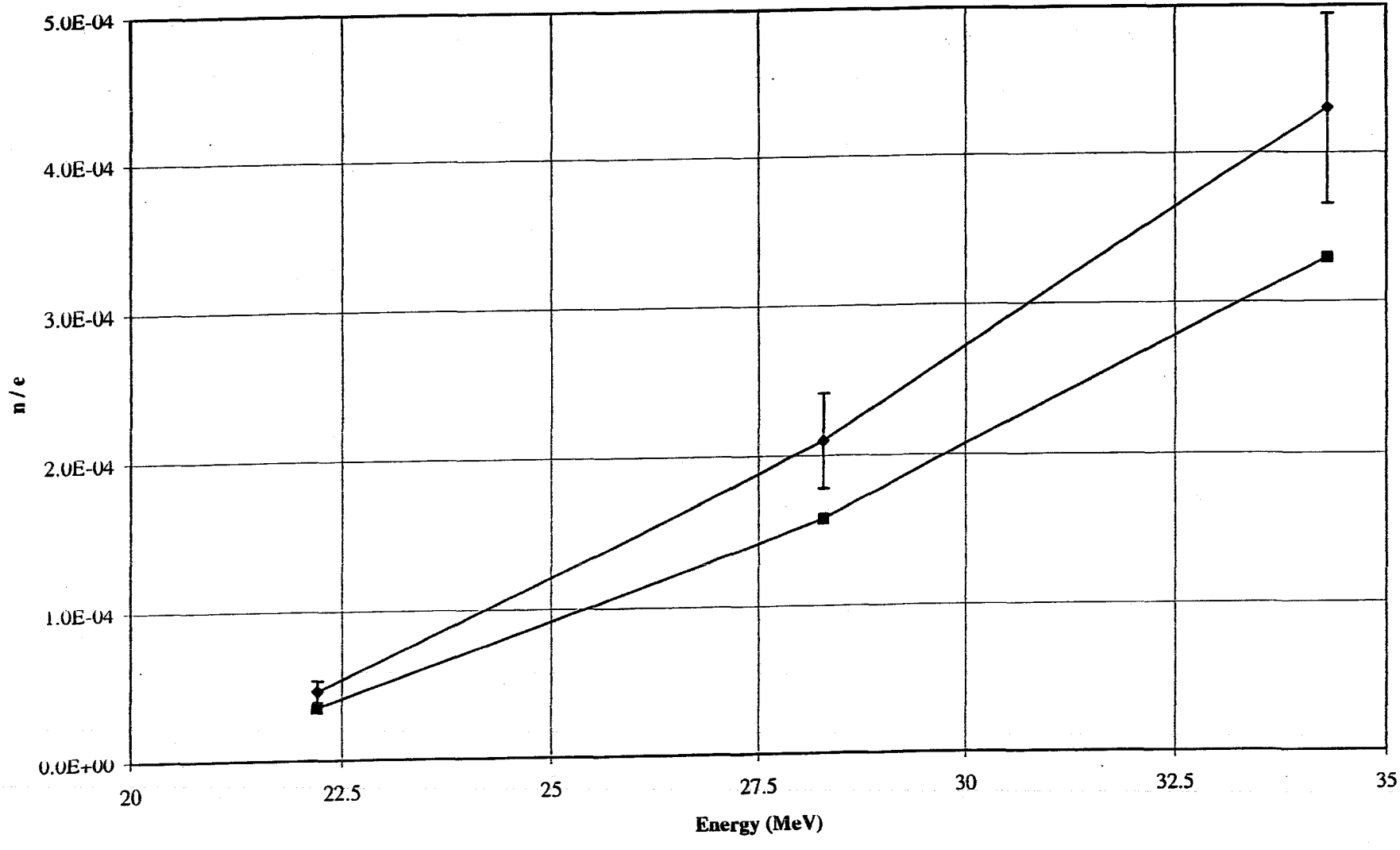

Figure 2. Neutron Yield per Electron Incident on the C-I Target

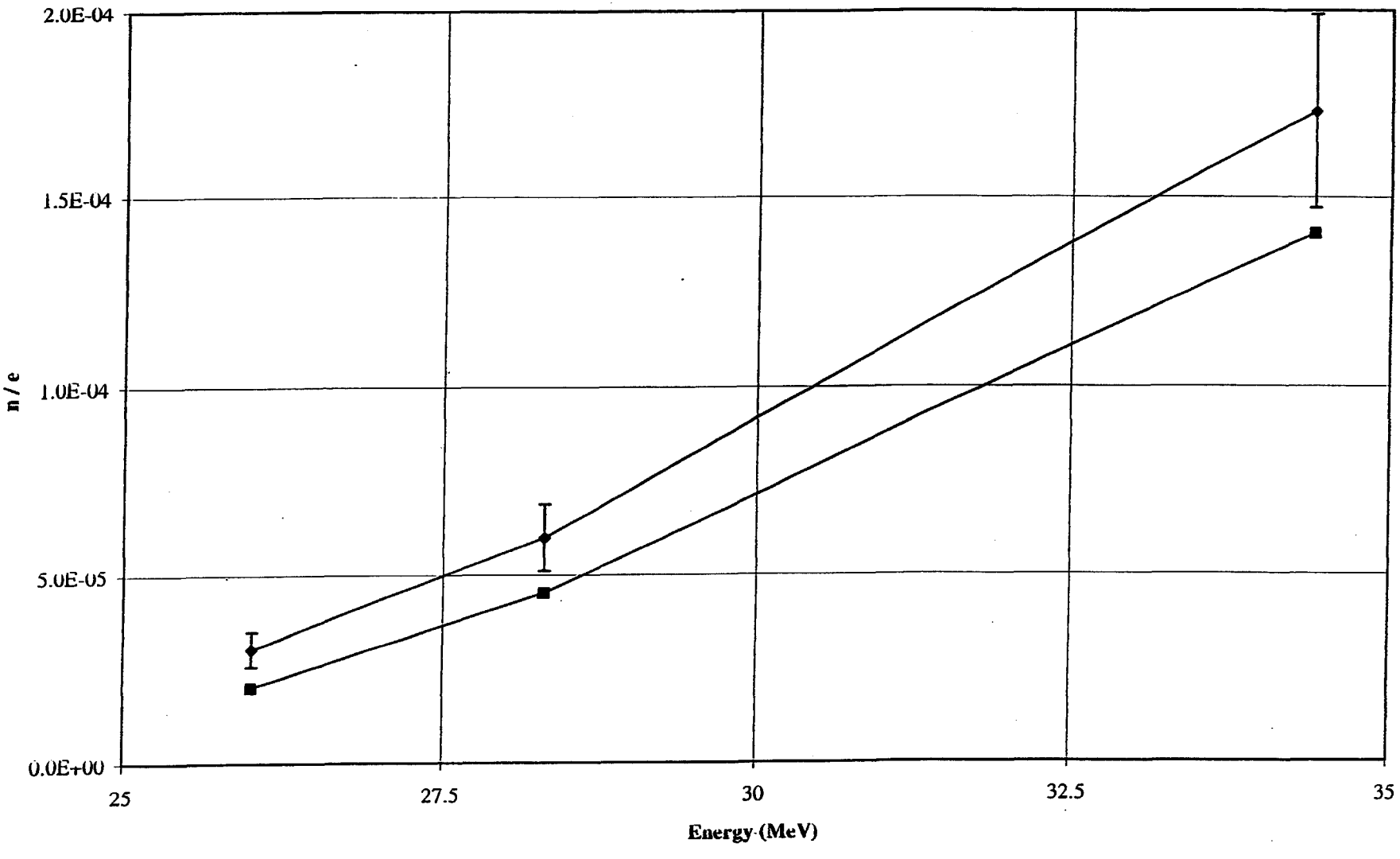

Figure 3. Neutron Yield per Electron Incident on the Pb-I Target

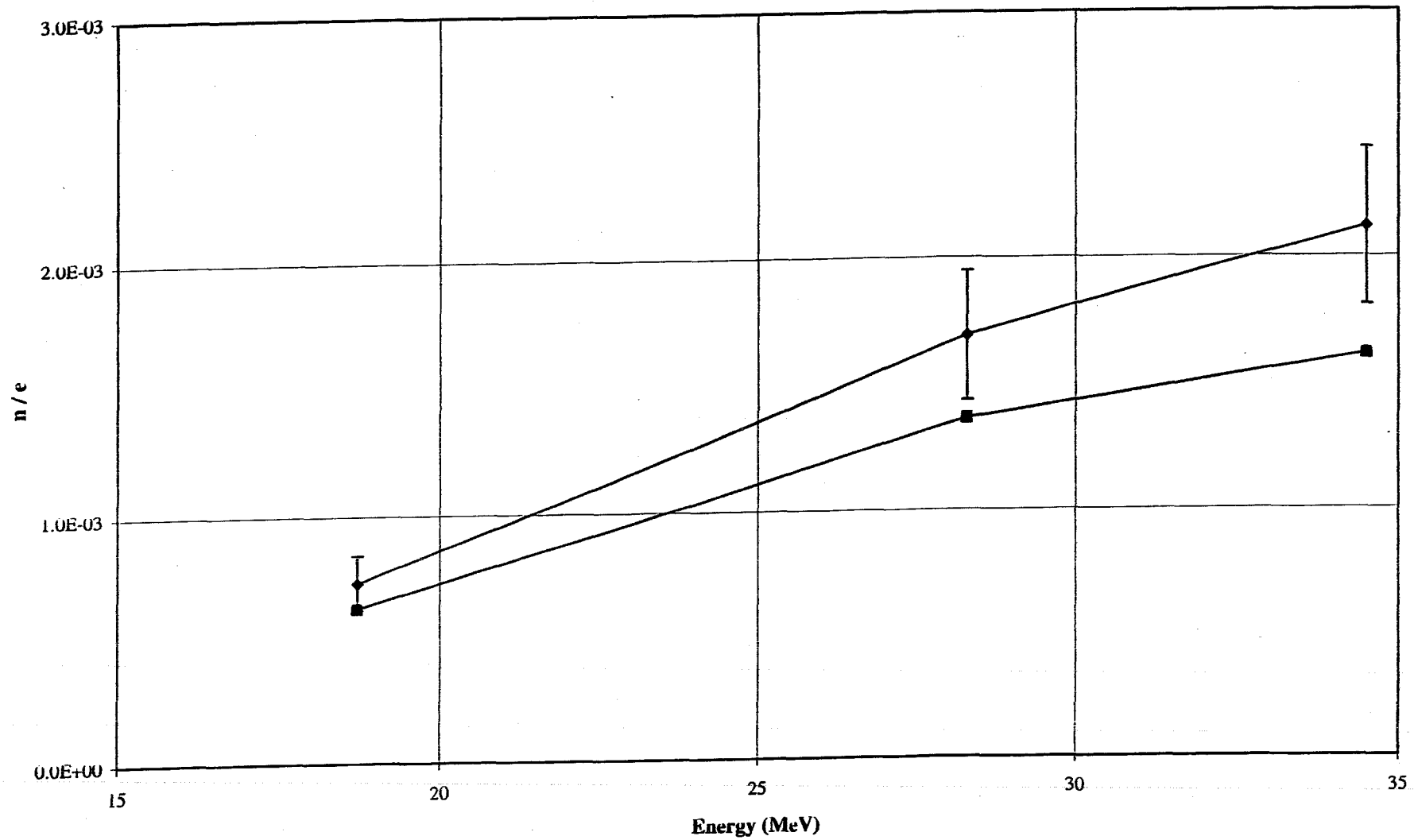

Figure 9. Neutron Yield per Electron Incident on the Pb-II Target

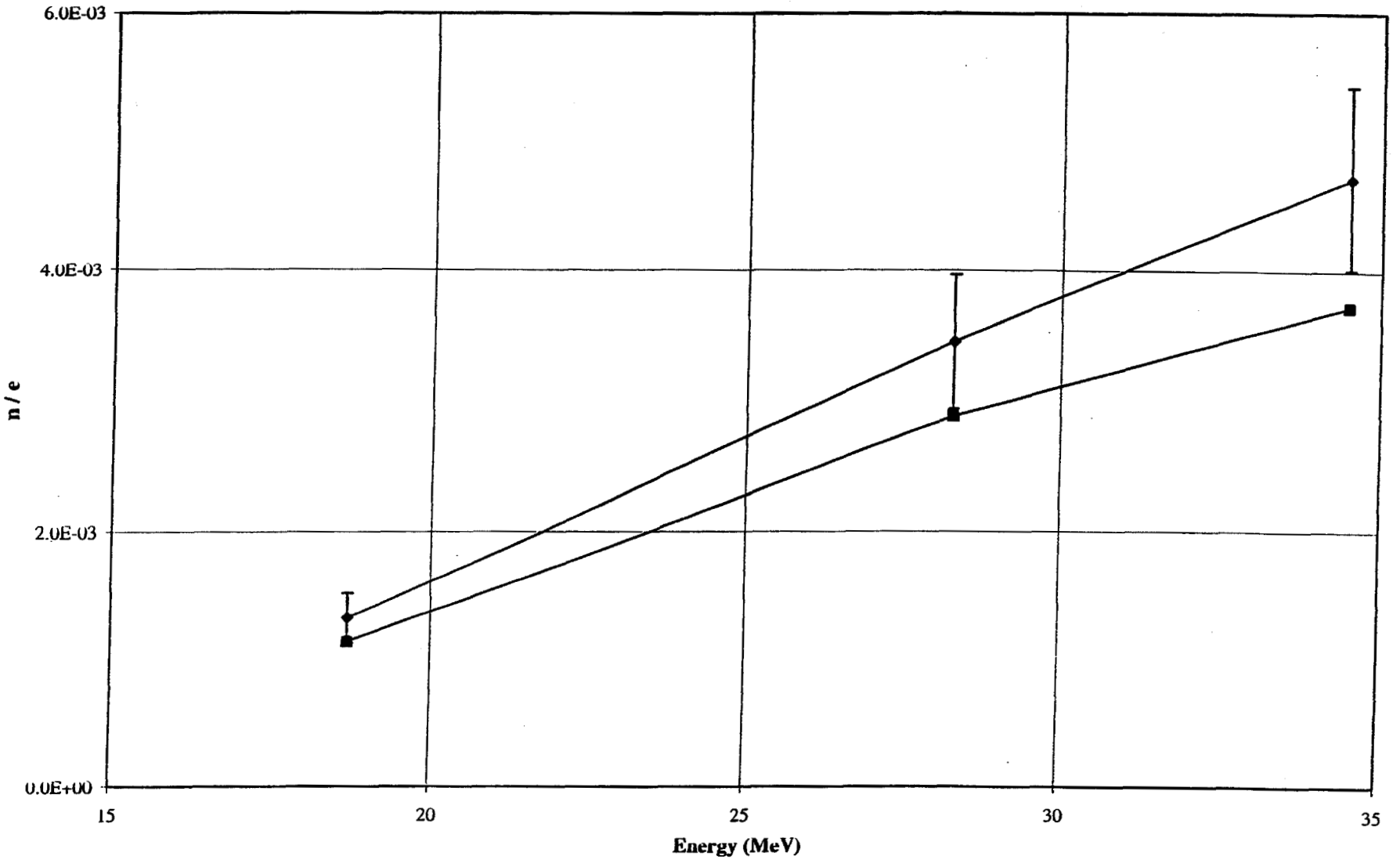

Figure 10. Neutron Yield per Electron Incident on the Pb-III Target

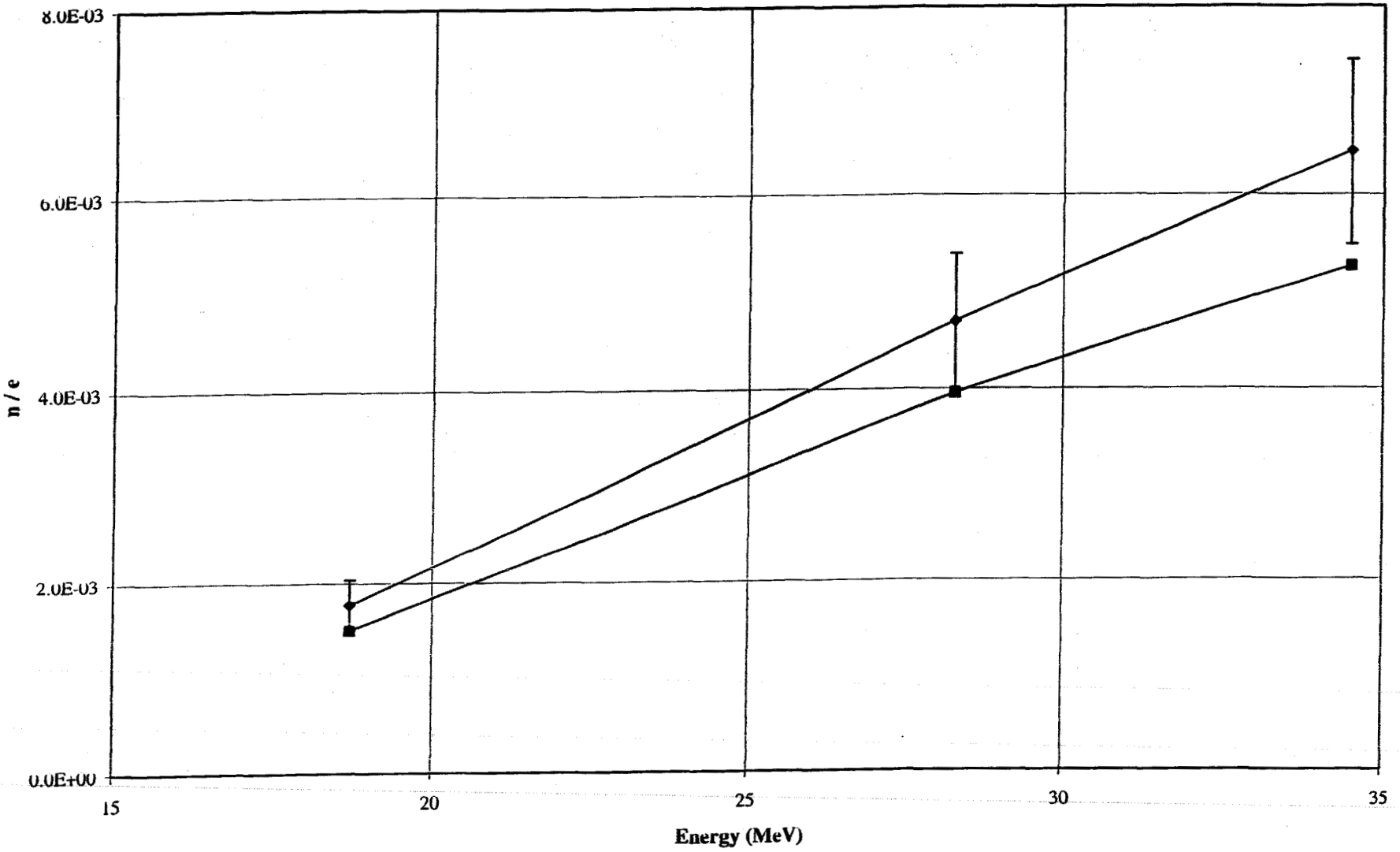

Figure 11. Neutron Yield per Electron Incident on the Pb-IV Target

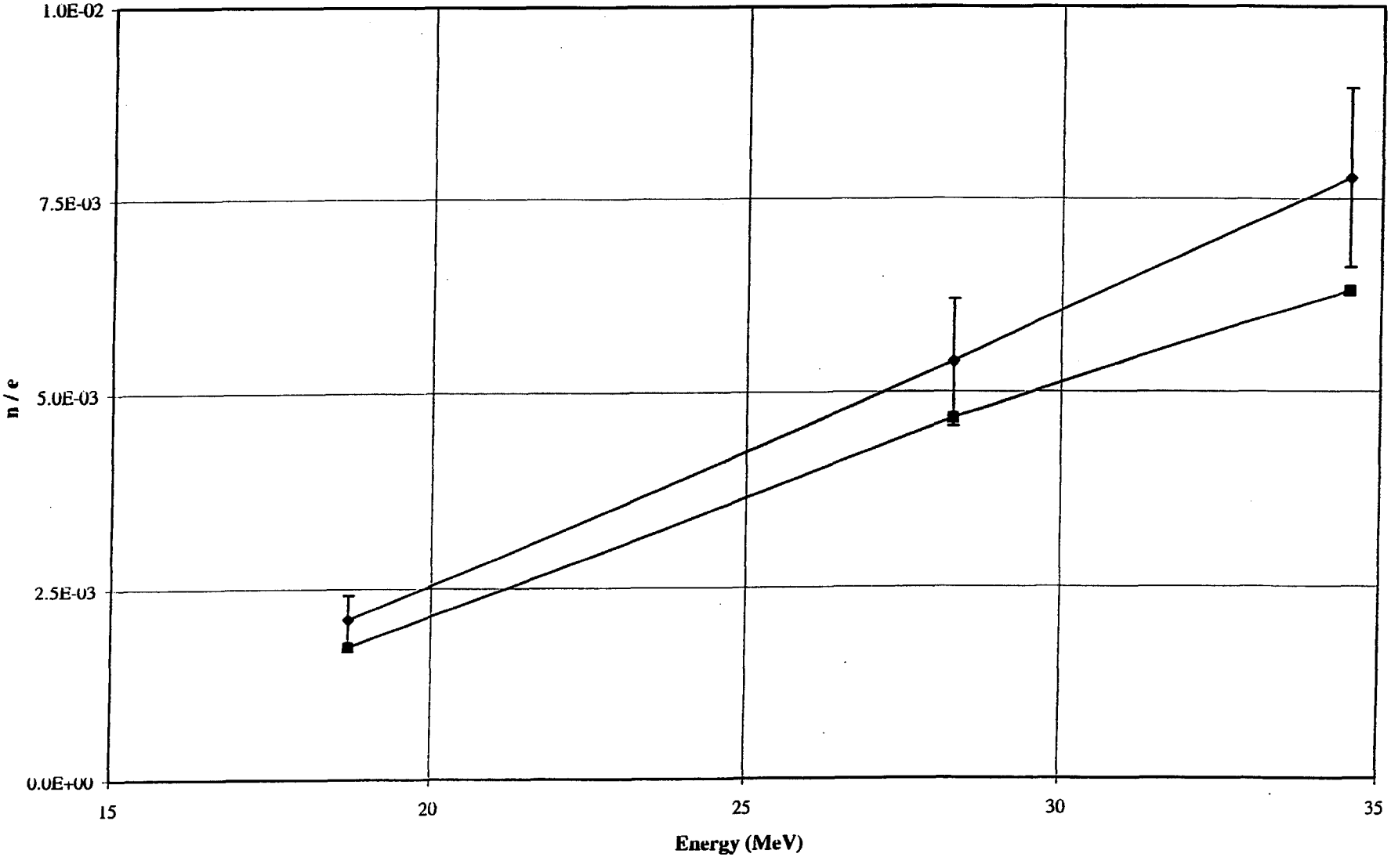

Figure 12. Neutron Yield per Electron Incident on the Pb-VI Target

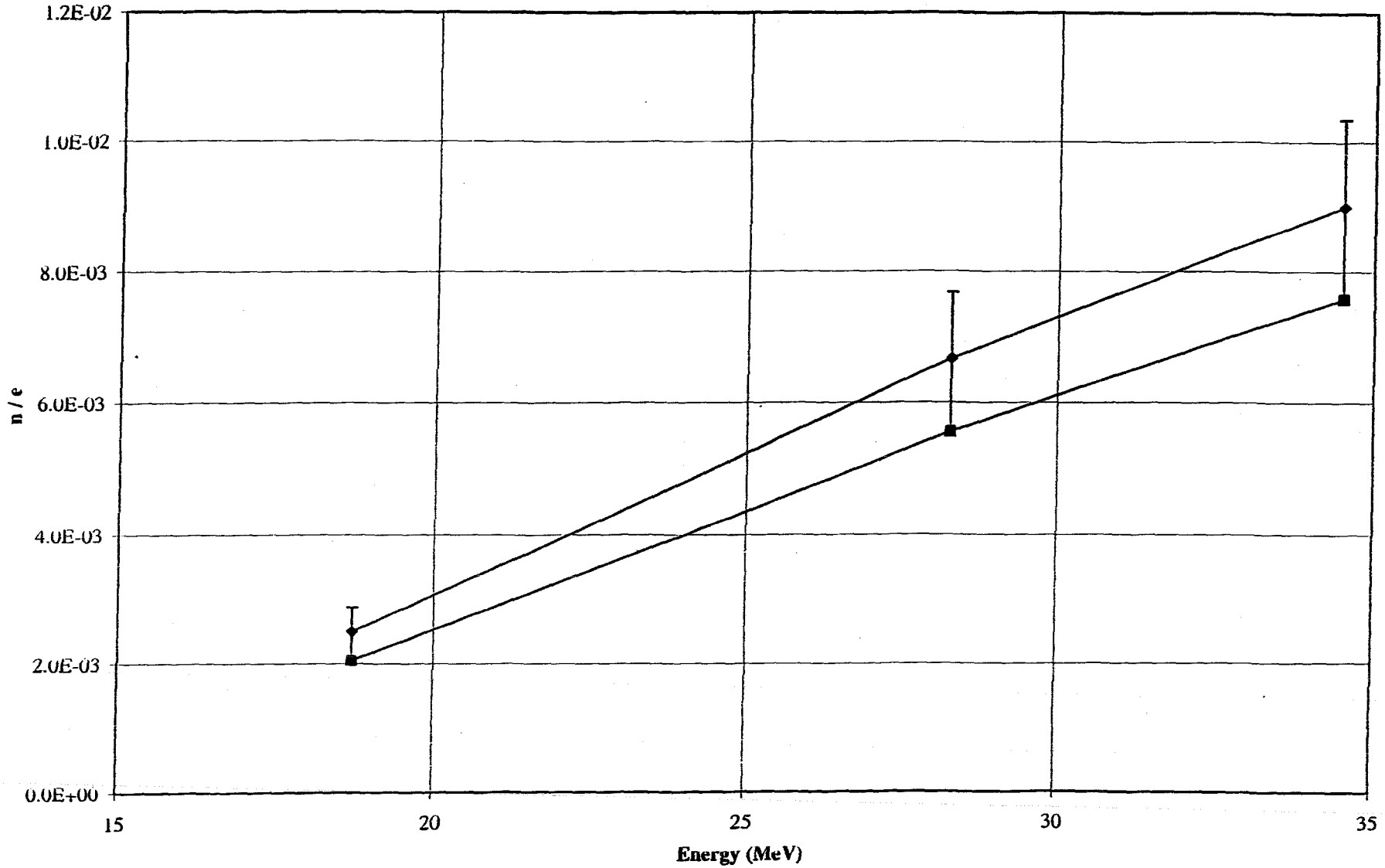

Figure 13. Neutron Yield per Electron Incident on the Ta-I Target

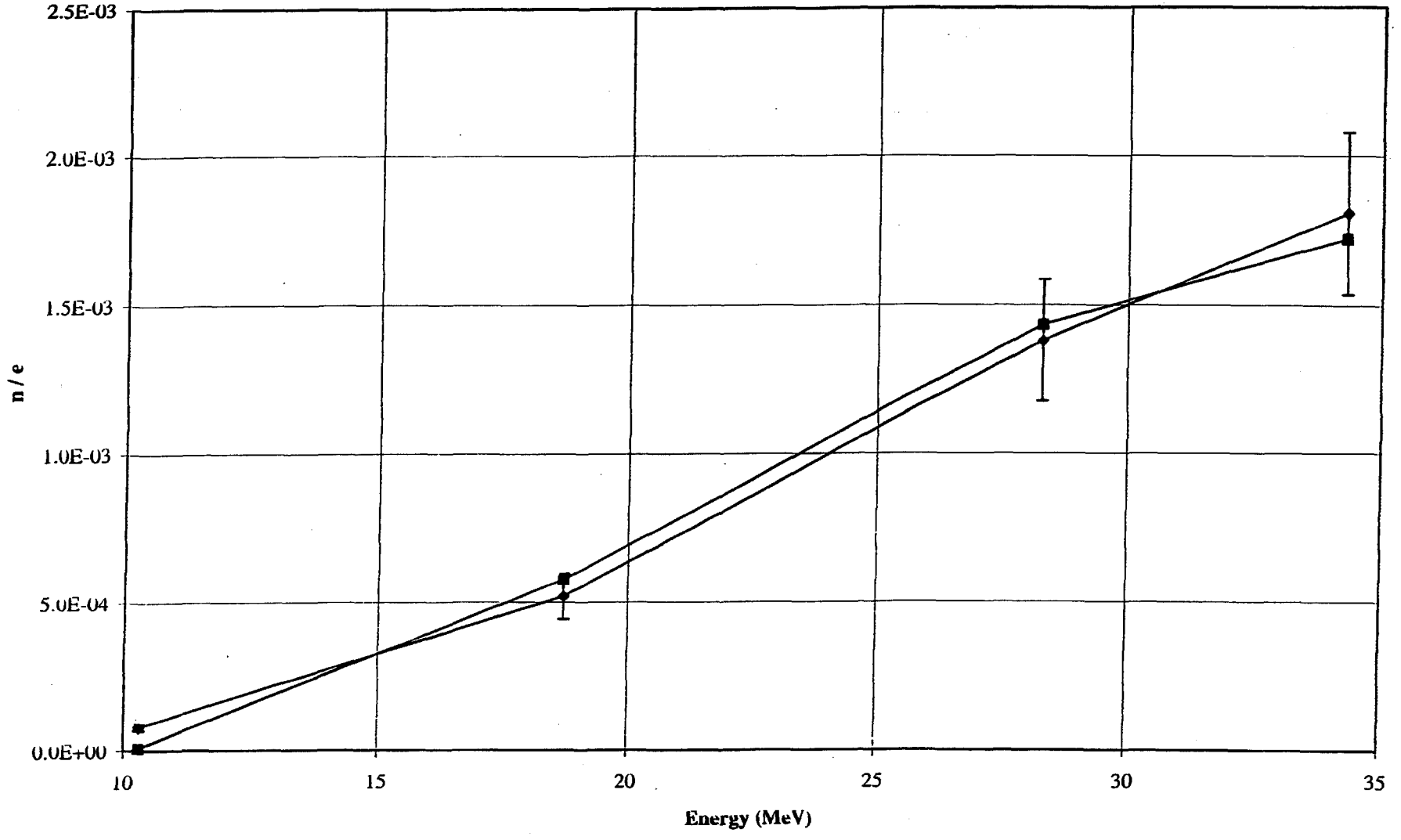

9

Figure 4. Neutron Yield per Electron Incident on the Cu-I Target

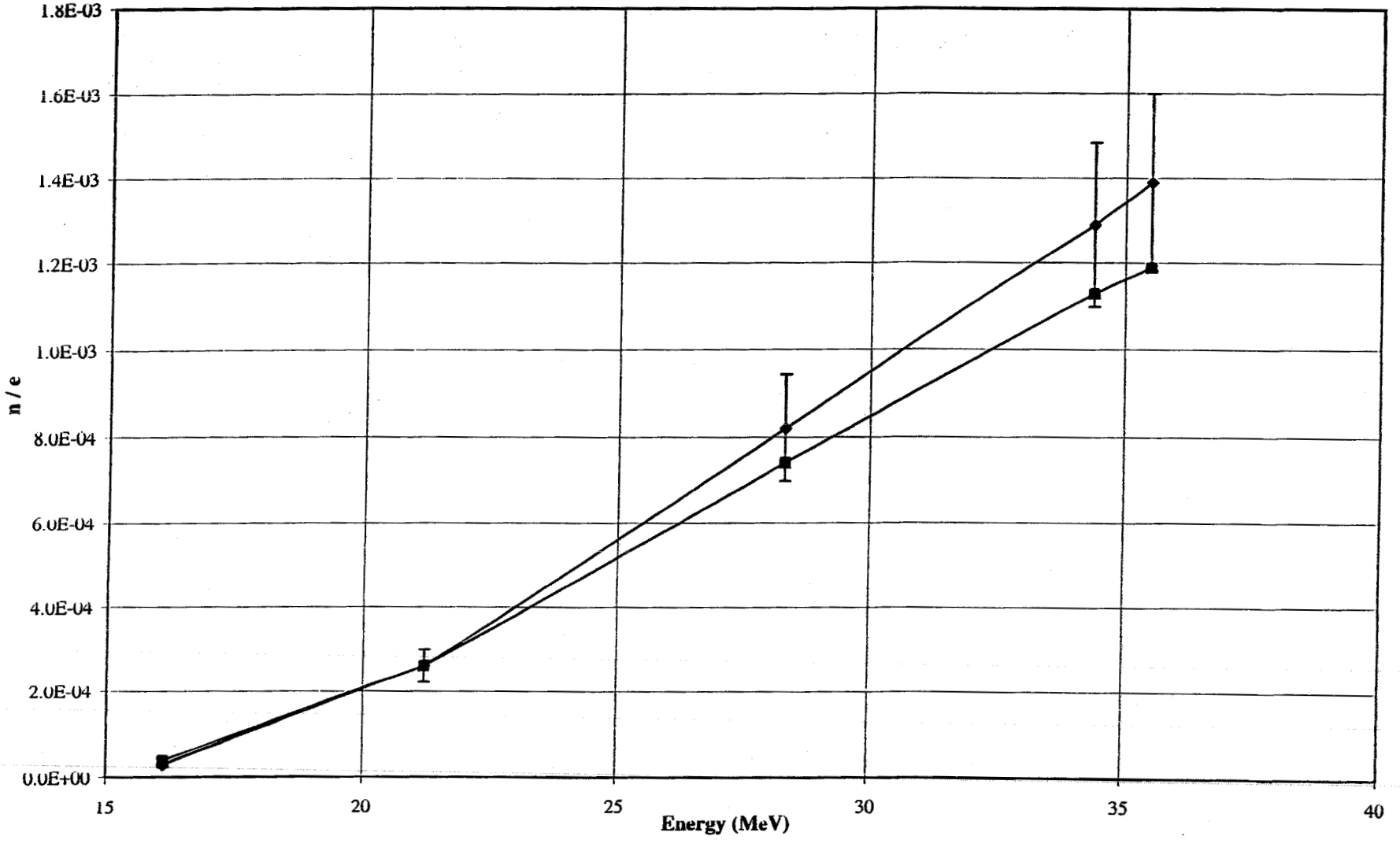

10

Figure 5. Neutron Yield per Electron Incident on the Cu-II Target

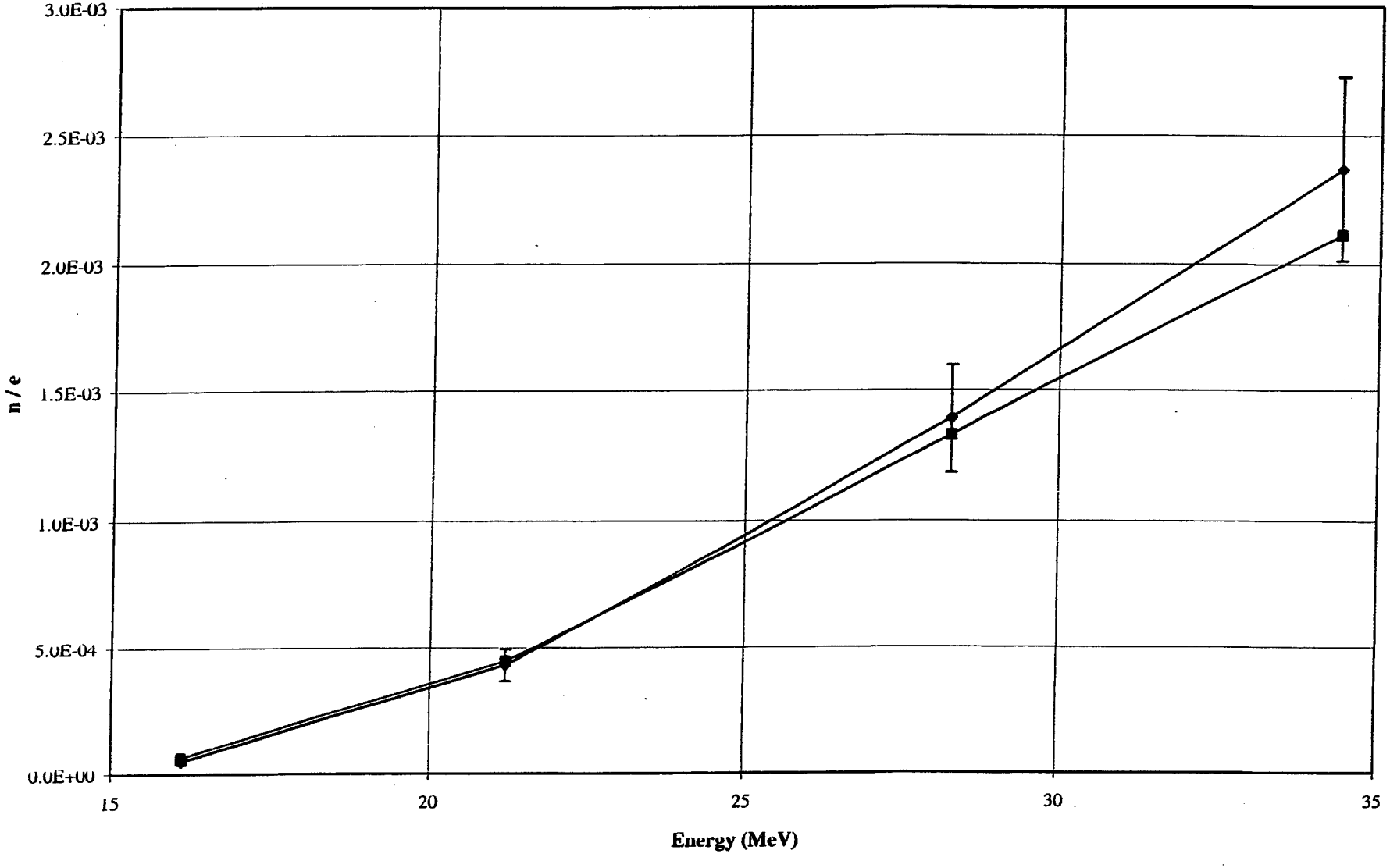

Figure 6. Neutron Yield per Electron Incident on the Cu-III Target

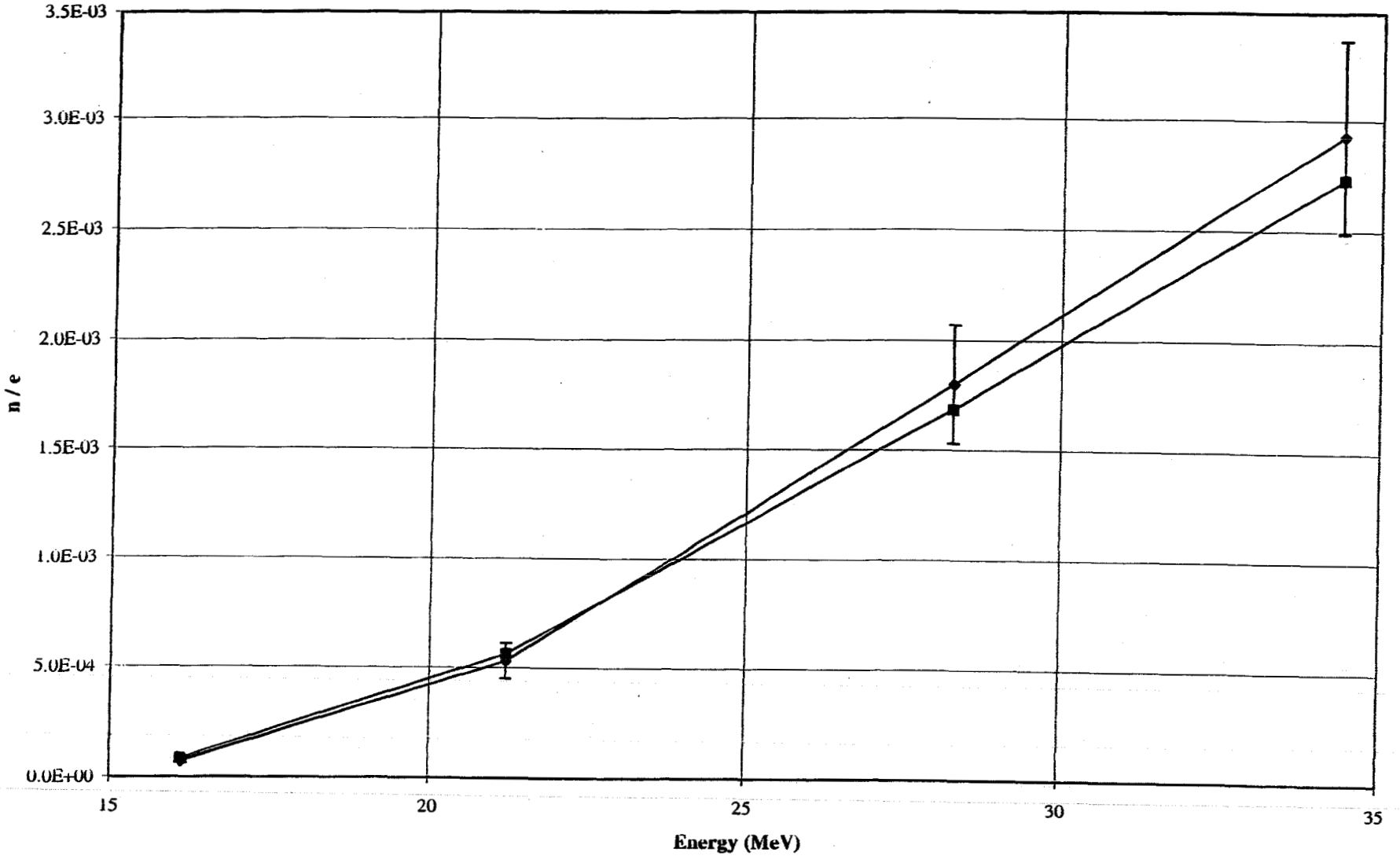

Figure 17. Neutron Yield per Electron Incident on the Cu-IV Target

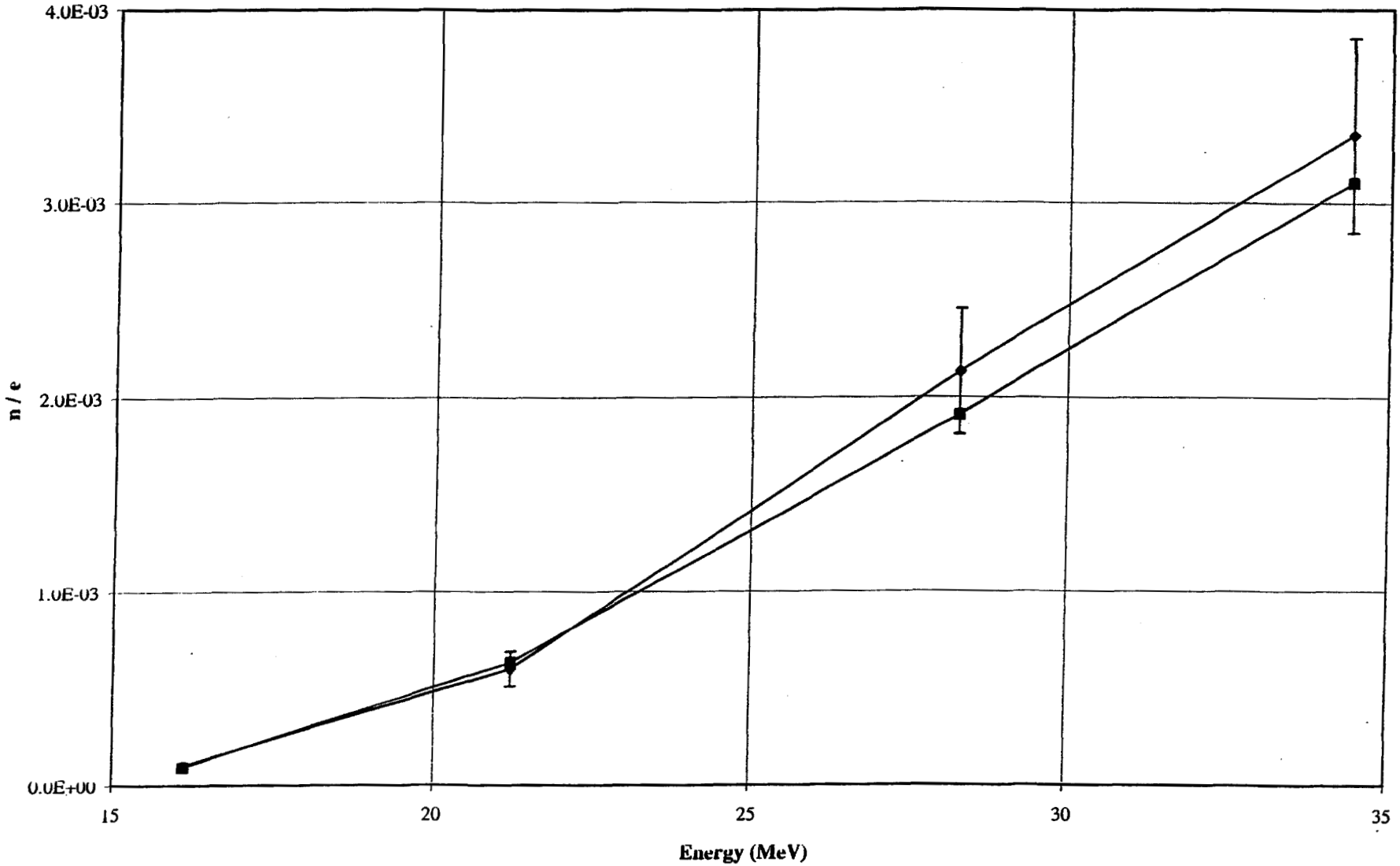

13

Figure 3. Neutron Yield per Electron Incident on the Cu-A Target

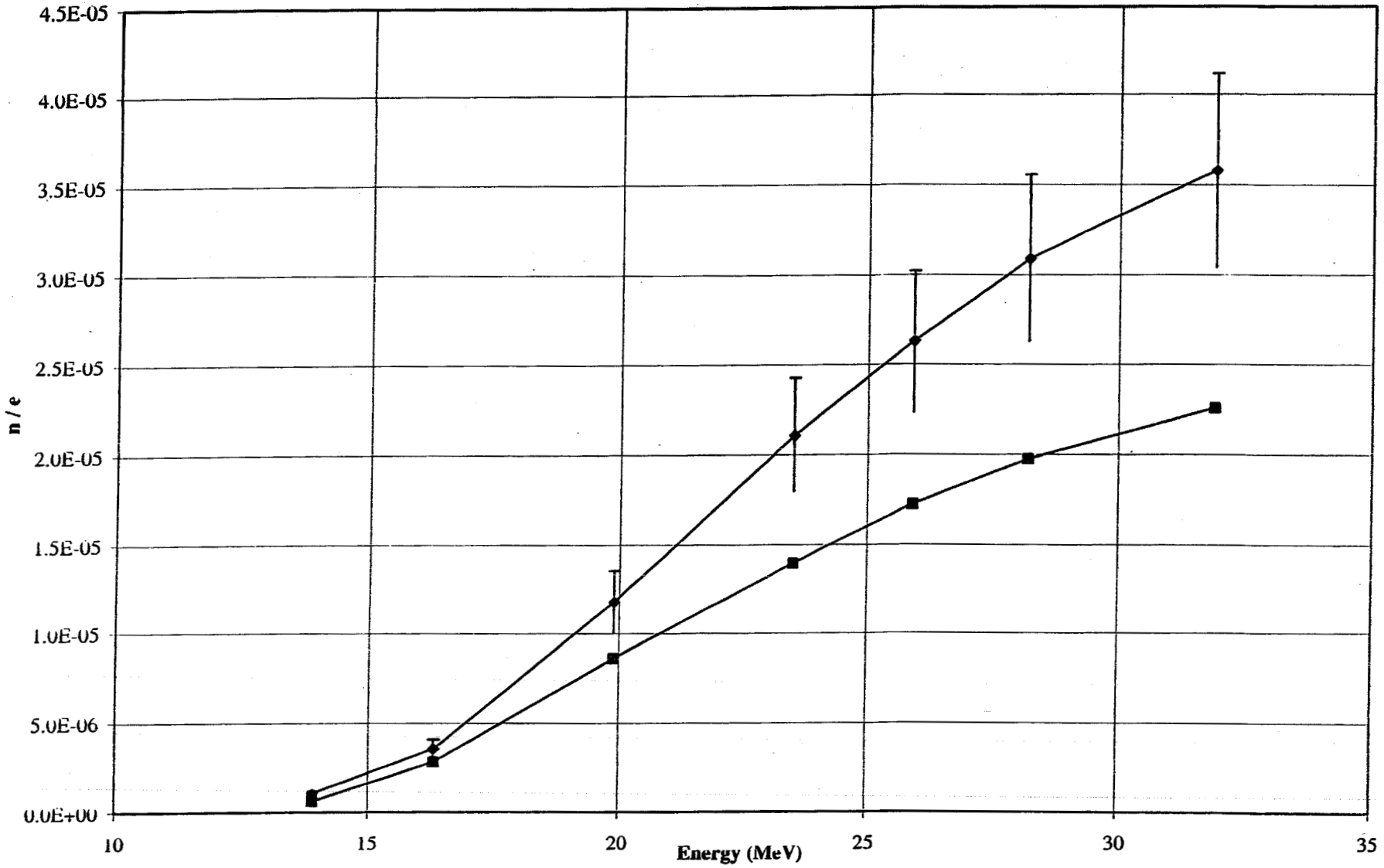

To be included as Appendix A.

Table A-1. Experimental and calculated values for the Al-I target.

Energy (MeV)	Exp. (n/e)	Calc. (n/e)	% Difference
22.2	4.60E-05	3.49615E-05	24%
28.3	2.10E-04	1.58349E-04	25%
34.3	4.30E-04	3.29464E-04	23%

Table A-2. Experimental and calculated values for the C-I target.

Energy (MeV)	Exp. (n/e)	Calc. (n/e)	% Difference
26.0	3.05E-05	2.04022E-05	33%
28.3	6.02E-05	4.51828E-05	25%
34.4	1.73E-04	1.40341E-04	19%

13

Table A-~~3~~. Experimental and calculated values for the Cu-A target.

Energy (MeV)	Exp. (n/e)	Calc. (n/e)	% Difference
13.9	1.08E-06	6.42411E-07	41%
16.3	3.55E-06	2.82607E-06	20%
19.9	1.18E-05	8.64947E-06	27%
23.5	2.11E-05	1.39760E-05	34%
25.9	2.63E-05	1.72198E-05	35%
28.2	3.09E-05	1.97438E-05	36%
31.9	3.58E-05	2.26232E-05	37%

9

Table A-~~4~~. Experimental and calculated values for the Cu-I target.

Energy (MeV)	Exp. (n/e)	Calc. (n/e)	% Difference
16.1	3.00E-05	3.93231E-05	-31%
21.2	2.60E-04	2.60412E-04	0%
28.3	8.20E-04	7.39411E-04	10%
34.4	1.29E-03	1.12818E-03	13%
35.5	1.39E-03	1.18875E-03	14%

10

Table A-~~5~~. Experimental and calculated values for the Cu-II target.

Energy (MeV)	Exp. (n/e)	Calc. (n/e)	% Difference
16.1	5.00E-05	6.59812E-05	-32%
21.2	4.30E-04	4.46299E-04	-4%
28.3	1.39E-03	1.32505E-03	5%
34.4	2.37E-03	2.11739E-03	11%

11

Table A-~~6~~. Experimental and calculated values for the Cu-III target.

Energy (MeV)	Exp. (n/e)	Calc. (n/e)	% Difference
16.1	7.00E-05	8.29270E-05	-18%
21.2	5.30E-04	5.62445E-04	-6%
28.3	1.80E-03	1.68784E-03	6%
34.4	2.93E-03	2.72927E-03	7%

Table A-7. Experimental and calculated values for the Cu-IV target.

Energy (MeV)	Exp. (n/e)	Calc. (n/e)	% Difference
16.1	1.00E-04	9.35682E-05	6%
21.2	6.00E-04	6.34144E-04	-6%
28.3	2.13E-03	1.91010E-03	10%
34.4	3.35E-03	3.10438E-03	7%

Table A-8. Experimental and calculated values for the Pb-I target.

Energy (MeV)	Exp. (n/e)	Calc. (n/e)	% Difference
18.7	7.30E-04	6.27176E-04	14%
28.3	1.69E-03	1.36643E-03	19%
34.5	2.12E-03	1.61103E-03	24%

Table A-9. Experimental and calculated values for the Pb-II target.

Energy (MeV)	Exp. (n/e)	Calc. (n/e)	% Difference
18.7	1.32E-03	1.13489E-03	14%
28.3	3.45E-03	2.87067E-03	17%
34.5	4.72E-03	3.71677E-03	21%

Table A-10. Experimental and calculated values for the Pb-III target.

Energy (MeV)	Exp. (n/e)	Calc. (n/e)	% Difference
18.7	1.77E-03	1.50326E-03	15%
28.3	4.69E-03	3.95314E-03	16%
34.5	6.46E-03	5.26382E-03	19%

Table A-11. Experimental and calculated values for the Pb-IV target.

Energy (MeV)	Exp. (n/e)	Calc. (n/e)	% Difference
18.7	2.10E-03	1.74783E-03	17%
28.3	5.37E-03	4.66777E-03	13%
34.5	7.77E-03	6.28967E-03	19%

Table A-12. Experimental and calculated values for the Pb-VI target.

Energy (MeV)	Exp. (n/e)	Calc. (n/e)	% Difference
18.7	2.50E-03	2.05297E-03	18%
28.3	6.67E-03	5.55570E-03	17%
34.5	9.00E-03	7.57502E-03	16%

Table A-13. Experimental and calculated values for the Ta-I target.

Energy (MeV)	Exp. (n/e)	Calc. (n/e)	% Difference
10.3	8.00E-05	8.18515E-06	90%
18.7	5.20E-04	5.77986E-04	-11%
28.3	1.38E-03	1.43330E-03	-4%
34.3	1.81E-03	1.72560E-03	5%